

A Comprehensive Study of Transformer Winding Losses Using the Finite Element Method

Peter Kosmatin¹, David Nedeljković²

¹Kolektor Etra, Šlandrova ulica 10, 1231 Ljubljana – Črnuče

²Univerza v Ljubljani, Fakulteta za elektrotehniko, Tržaška 25, 1000 Ljubljana, Slovenija

E-pošta: davidn@fe.uni-lj.si

Abstract. The paper presents a study of the transformer winding losses caused by eddy and circulating currents using the finite element method. The losses are evaluated using different transformer simulation models and by including the phase interaction effect. The increase in the winding losses is also evaluated when the transformer is exposed to geomagnetically induced currents. A new calculation method using a 2D axisymmetric geometry is proposed. In comparison with a 3D simulation model based on detailed manufacturing data for 14 power transformers, the proposed procedure demonstrates an acceptable level of accuracy, achieved within a short computational time. Consequently, this method can be used as a valuable design tool for optimising the transformer geometry.

Keywords: Eddy currents, circulating currents, geomagnetically induced currents, finite element analysis, power transformers

Študija izgub v navitjih transformatorja z uporabo metode končnih elementov

V prispevku je predstavljena študija izgub v navitjih transformatorja, ki jih povzročajo vrtilni in krožni tokovi, z uporabo metode končnih elementov. Izgube so ovrednotene z uporabo različnih simulacijskih modelov transformatorjev in z vključitvijo učinka fazne interakcije. Povečanje izgub v navitju se je ocenilo tudi za primere, ko je transformator izpostavljen geomagnetno induciranim tokovom. Posledično je predlagana nova metoda izračuna z uporabo 2D osnosimetrične geometrije. Za ovrednotenje metode je bila opravljena primerjava njenih rezultatov z rezultati 3D simulacijskega modela, zgrajenega na podlagi podrobnih proizvodnih podatkov za 14 projektiranih in izdelanih energetskih transformatorjev. Primerjava kaže, da predlagana metoda zagotavlja sprejemljivo natančnost s kratkim računskim časom, zato se lahko uporablja kot učinkovito načrtovalsko orodje za optimizacijo geometrije transformatorja.

Ključne besede: Vrtilni tokovi, geomagnetno inducirani tokovi, krožni tokovi, metoda končnih elementov, energetski transformatorji

1 INTRODUCTION

Due to the longevity of power transformers, their high operating efficiency is of paramount importance. As transformer power and voltage ratings increase, the accurate estimation of losses during the design process

becomes increasingly crucial. To ensure competitiveness on the global market, transformer manufacturing companies must optimise their designs within technical and technological limitations [1, 2]. This involves optimising not only the quantity of installed materials but also the mathematical models employed to predict the parameters of the constructed transformer. The key parameter guaranteed by the manufacturer after signing a construction contract with a customer is the value of the short-circuit losses during a normal transformer operation.

High-power transformer design incorporates an iterative geometry optimisation procedure, using a previously manufactured transformer with similar characteristics as a starting point. Although some design optimisation algorithms have been found among the published papers [3-7], the product uniqueness forces power transformer designers to rely on their experience and the established design methods within the company. With each modification of the transformer geometry, numerous calculations must be performed to verify the transformer compliance with the adopted technical specifications and the corresponding standards. Besides their accuracy, the calculation methods must be time-efficient to optimise the design process. The paper addresses one of the calculation procedures and presents a basis for evaluating additional load losses on a given transformer geometry under various operating conditions.

The load losses are the most dominant component

Received: 20 March 2025

Accepted: 21 April 2025



Copyright: © 2025 by the authors
Creative Commons Attribution 4.0
International License

with the values of approximately 80% of the dissipated high-power transformer electromagnetic losses. Their predominant portion is generated within the transformer windings, where losses can be categorised into two specific types: direct current (DC) ohmic losses and stray losses, the latter arising from leakage fields. The stray losses can be further divided into eddy current losses and circulating current losses present where the winding is constructed with parallel conductors to reduce the eddy current losses. Any additional losses, such as the skin-effect losses, are negligible in the total winding losses of a high-power transformer [8]. The first step in assessing the stray winding losses is to determine the leakage field distribution within the transformer windings. Typically, an analytical approach is used that achieves a satisfactory balance between the accuracy and computational efficiency [9, 10]. Nowadays, when computers with a high computational power are available to transformer designers, the numerical finite elements method (FEM) for leakage field calculations can be included within the design procedure. The applicability of FEM in the transformer design is well documented in [11-14], however, a practical geometry meshing is required to achieve an acceptable computational speed, especially when the geometry is modelled in a 3D space. Bearing this in mind, this study focuses on finding a suitable winding stray losses calculation procedure using an FEM-based computer software (Ansys Maxwell [15], FEMM [16]). Such a procedure can then be used in the transformer design optimisation process. A comparison is made between various 2D and 3D transformer modelling possibilities, taking into account their accuracy and computational speed. The evaluation is made on a sample of 14 transformers of a rated power from 10 MVA to 500 MVA.

The winding losses are also calculated at the presence of geomagnetically induced currents (GIC) [17-19] which occur when the geomagnetic disturbance affects the distribution of the electric potential on the Earth surface, resulting in a flow of induced currents in low-resistance paths that include transmission lines coupled to neutral-grounded transformer windings. For a transformer operating at 50 Hz, GIC with a low frequency (a few mHz) can therefore be treated as a DC source. The presence of GIC flowing through the transformer windings can lead to a high saturation of the core, resulting in the distortion of the stray magnetic field inside the transformer [20-23]. Consequently, the winding stray losses increase and the hot-spot temperature rises as well [24]. The simulated values of the injected GIC into the transformer model are based on the measurements [25], where the maximum GIC value of 67 A per phase is measured in the Finnish power system.

2 STRAY LOSSES OF THE TRANSFORMER WINDINGS

A time-varying leakage field is formed when the transformer windings are not perfectly coupled and some of the magnetic flux generated by the load currents is distributed within the windings and outside the core. While some leakage field is usually needed to limit the fault currents, it causes stray losses in the exposed conductive materials (windings, tank, clamps, etc.).

For the leakage field calculation, analytical methods have been developed [9]. They are commonly used in the initial transformer design. However, for an accurate determination of the magnetic field distribution, a 3D mathematical model is developed [26] and enhanced with FEM-based computer programs.

Using Ansys Maxwell as a field calculation tool, designers have several choices of how to construct the transformer model, either a 2D or a 3D model, with the former offering an axisymmetric or *xy*-plane option. With FEMM, a freeware program, only 2D modelling is supported. The options will be compared later, below in terms of their accuracy and computational speed.

2.1 Eddy Current Losses

When the distribution of the magnetic field for a given transformer geometry is known, the winding eddy current losses can be evaluated analytically. The classical approach can be used, where the conductor is described as an infinitely long strand (Figure 1). A strand with a rectangular cross-section is affected by external magnetic field H_y [9, 10]. By applying the Maxwell's equations, the magnetic field distribution in the strand obtained by the diffusion equation is:

$$\frac{\partial^2 H_y}{\partial x^2} = \mu\sigma \frac{\partial H_y}{\partial t}, \quad (1)$$

where μ and σ are the permeability and conductivity of the strand material, respectively. Due to the load current and GIC, the time and spatial dependence of external magnetic field H_y has the following form:

$$H_y(x, t) = \hat{H}_0(x)e^{j\omega t} + H_{GIC}(x). \quad (2)$$

Where \hat{H}_0 is the peak value of the sinusoidal magnetic field waveform due to the load current, and H_{GIC} is the magnetic field DC value due to GIC. For solving (1), the magnetic field boundary condition on either side of the conductor is:

$$H_y\left(\pm \frac{b}{2}, t\right) = \hat{H}_0 e^{j\omega t} + H_{GIC}. \quad (3)$$

Due to the small dimensions of the conductor, peak sinusoidal magnetic field \hat{H}_0 at the conductor centre can be used, or it can be calculated as a mean value between the readings on either side of the conductor. Therefore, magnetic field distribution H_y within a conductor is:

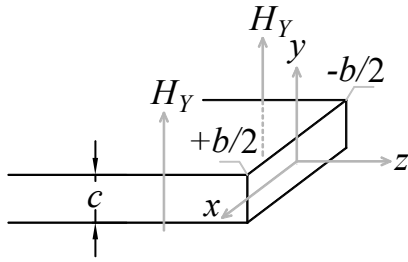


Figure 1. Rectangular strand in an external magnetic field with a y -component [9].

$$H_y(x, t) = H_{GIC} + \hat{H}_0 e^{j\omega t} \frac{\cosh(j\omega\mu\sigma x)}{\cosh\left(j\omega\mu\sigma \frac{b}{2}\right)}. \quad (4)$$

The generated eddy current losses are then calculated using the ohmic loss component of the Poynting theorem:

$$P_{eddy} = \int_V \mathbf{J} \cdot \mathbf{E} dv = \frac{1}{\sigma} \int_V \mathbf{J}^2 dv = \frac{1}{2\sigma} \int_V |\hat{\mathbf{J}}|^2 dv. \quad (5)$$

Based on the presented electromagnetic problem in Figure 1 with current density \mathbf{J} having only the z -component, the eddy current losses per unit length (l) in the z -direction are expressed as:

$$\begin{aligned} \frac{P_{eddy}}{l} &= \frac{c}{2\sigma} \int_{-\frac{b}{2}}^{+\frac{b}{2}} \left| \frac{\partial H_y}{\partial x} \right|^2 dx = \\ &= \frac{c |j\omega\mu\sigma|^2 |\hat{H}_0 e^{j\omega t}|^2}{2\sigma \left| \cosh\left(j\omega\mu\sigma \frac{b}{2}\right) \right|^2} \int_{-\frac{b}{2}}^{+\frac{b}{2}} |\sinh(j\omega\mu\sigma x)|^2 dx = \quad (6) \\ &= \frac{c \cdot q \cdot \hat{H}_0^2}{\sigma} \left[\frac{\sinh(qb) - \sin(qb)}{\cosh(qb) + \cos(qb)} \right]. \end{aligned}$$

Where q is the reciprocal value of the skin depth:

$$q = \sqrt{\frac{\omega\mu\sigma}{2}}, \quad (7)$$

while c and b are the strand dimensions. Besides the skin depth, the argument in the trigonometric and hyperbolic functions is the strand dimension perpendicular to the direction of external magnetic field H_y . The eddy current losses are commonly expressed per a unit volume and written separately for the axial $\hat{H}_{0,z}$ and radial $\hat{H}_{0,r}$ component of the magnetic field (polar coordinate system):

$$\begin{aligned} \frac{P_{eddy,z}}{V} &= \frac{q \cdot \hat{H}_{0,z}^2}{\sigma \cdot c} \left[\frac{\sinh(qc) - \sin(qc)}{\cosh(qc) + \cos(qc)} \right]; \\ \frac{P_{eddy,r}}{V} &= \frac{q \cdot \hat{H}_{0,r}^2}{\sigma \cdot b} \left[\frac{\sinh(qb) - \sin(qb)}{\cosh(qb) + \cos(qb)} \right]. \end{aligned} \quad (8)$$

Even though the external magnetic field has an additional DC component due to GIC (2), the eddy current losses depend only on the time-varying

magnetic field component. To eliminate the DC bias, it is necessary to obtain a half of the peak-to-peak magnetic field affecting the conductor. Therefore, the equation (8) can be used. The total winding eddy current losses can then be calculated as a sum of all (N) individual conductor losses:

$$P_{eddy} = \sum_{i=1}^N \left(\frac{P_{eddy,r}}{V}(i) + \frac{P_{eddy,z}}{V}(i) \right). \quad (9)$$

For the windings with a low number of turns that carry a high-load current, there is also a considerable azimuthal component of eddy current losses [27]. Based on the given reference, the azimuthal eddy current losses can be neglected for the transformers of the disk type or the multiple-layer type coils. The 14 transformers, for which the additional winding losses are evaluated, are constructed with these coil types. Consequently, the azimuthal eddy current losses are neglected.

Another aspect to consider when modelling the transformer and calculating the magnetic field is the interaction between the phases. Leakage magnetic field H_i imposed on the conductor is the vector sum of the fields formed by the adjacent phases:

$$\begin{aligned} H_i &= \hat{H}_0 \cdot e^{j\omega t} + a \cdot \hat{H}_0 \cdot e^{j\left(\omega t \pm \frac{2\pi}{3}\right)} \\ \left| \frac{\hat{H}_i}{\hat{H}_0} \right|^2 &= 1 - a \cdot \left(e^{\pm j\frac{2\pi}{3}} + e^{\mp j\frac{2\pi}{3}} \right) + a^2 = 1 - a + a^2, \quad (10) \\ &\quad \left. \begin{array}{l} 2 \cdot \cosh\left(j\frac{2\pi}{3}\right) = \\ = 2 \cdot \cos\left(\frac{2\pi}{3}\right) = 1 \end{array} \right\} \end{aligned}$$

where a is the magnetic leakage field modification parameter due to the phase interaction. Its value depends on the specific position of the conductor and varies around its circumference. As the conductor is affected by the cosine function of the magnetic leakage field, the peak radial field value would be expected at a 0° phase angle along the entire length of the conductor. However, due to the interaction of the adjacent phase, the phase angle of the peak magnetic leakage field varies around the circumference of the conductor, as shown in the example, given in Figure 2. Therefore, to increase the accuracy of the eddy current losses calculation, the winding must be segmented along its circumference, and the equation (8) can be used correctly.

2.2 Circulating Current Losses

The value of the ohmic and eddy current losses is highly dependent on the dimensions of the conductors that carry the high current. In order to reduce the ohmic losses, it is therefore necessary to divide the conductor into parallel strands, while maintaining the overall cross-section of the conductor. As a result, the circulating currents can occur if there is no proper transposition between the parallel conductors.

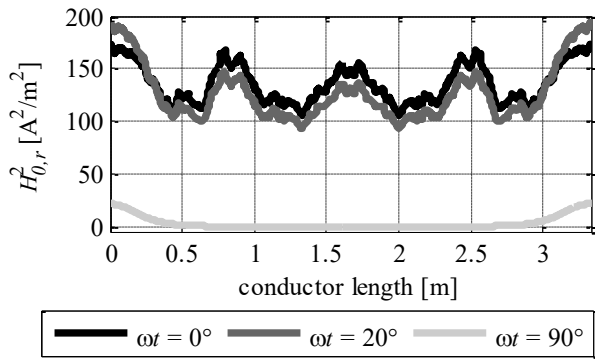


Figure 2. Radial component of the magnetic leakage field at a given phase angle around a particular conductor circumference (example).

An ideal transposition ensures that the parallel conductors share the same amount of the magnetic leakage field and therefore there is no current circulation. Analytical [28, 29] or numerical [9, 30] methods can be used to evaluate the circulating current losses with a particular transposition scheme. In high-power transformers, the circulating losses are usually focused to the low-voltage winding, and even there only if a continuously transposed cable is not used.

In this paper, the currents through the n_p parallel conductors with a transposition scheme shown in Figure 3 are numerically calculated. The winding scheme shown with n_p-1 transpositions is relatively easy to construct and it the windings are assumed to be placed centrally on the limb.

A transformer with parallel conductors is modelled in a 2D space according to the used transposition (Figure 4). The short-circuit test is analyzed with a rated current excitation on the high-voltage winding, and the circulating current losses are calculated.

3 RESULTS AND DISCUSSION

The simulations are carried out on a set of 14 transformers, with their data provided in Table 1. The values are provided by the power transformer manufacturer along with a detailed geometry and material specification.

3.1 Eddy Current Losses of the Transformer Windings

To calculate the winding eddy current losses, a high-power five-limb transformer (Transformer no. 12 in Table 1) is modelled in a 3D space (Figure 5). Besides the core and the winding elements, the model includes most of the installed conductive components, such as tie plates, clamps and tank shunts, which further affect the distribution of the stray field inside the transformer. Despite using the surface impedance boundary conditions [11], the model requires a dense finite element mesh for an accurate magnetic field calculation.

Table 1: Rated values of the analysed transformers

Tr. no.	Rated power [MVA]	Rated voltage HV/LV [kV/kV]	Ohmic losses [kW]
1	10	115/38.5	37.7
2	16	46/23	69.2
3 ^a	25	138/22	54.6
4 ^a	27.5	115/10.5	59.4
5 ^a	30	48/23	78.2
6 ^a	40	132/22	83.0
7 ^a	50	135/23	96.3
8	63	140/46	174.7
9	90	132/33	182.9
10	100	132/10.5	252.7
11	125	330/115	302.2
12 ^b	300	400/115	458.5
13 ^b	350	400/121	480.5
14 ^b	500	415/145	758.5

In the presence of a voltage regulation winding, a transformer is simulated at the rated tap position.

^a Transformer with the coils wound with rectangular parallel conductors

^b Five-limb transformer

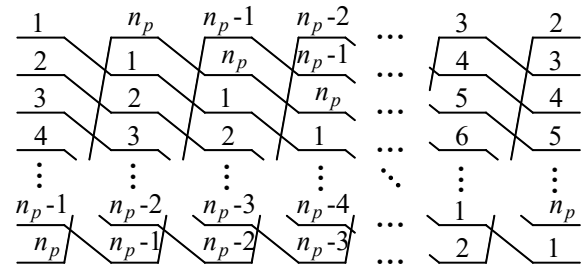


Figure 3. Transposition scheme for the n_p parallel conductors.

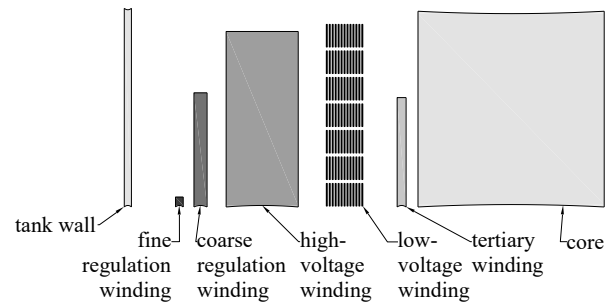


Figure 4. In-plane 2D transformer model for circulating currents evaluation.

While the transformer length, height and depth may be several metres, at least one dimension of the constructed elements is in the range of a few tens of millimetres. Meshing and analysing such a model is a demanding task, even for a high-end specialised personal computer. Since modelling with long magnetic field computation time is impractical for the transformer design optimisation, a simplified 3D model including a core, windings and tank without magnetic shunts is built.

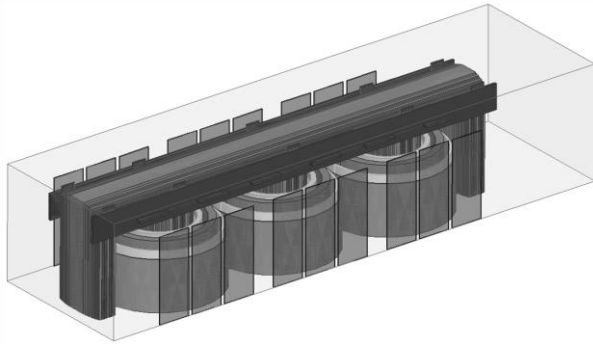


Figure 5. Top half of the detailed 3D transformer model.

Due to the symmetry of the transformer, it is sufficient to model only its ¼, thus reducing the mesh size. In order to evaluate the reduced accuracy resulting from the model simplifications, both a detailed and a simplified model of the transformer no. 12 (Table 1) are built.

Because of the small difference between the calculated total eddy current losses of the two models (Table 2), the simplified version can be used. Due to the large ohmic loss component (458.5 kW in Table 1), such a decision is even more justified when the total winding losses are evaluated.

With the Ansys Maxwell adaptive meshing, the number of the finite elements for the model analysis to converge to the targeted energy error is roughly five times higher for the detailed transformer model ($1.8 \cdot 10^6$ finite elements). Although the number of the finite elements is greatly reduced within the simplified model, the relatively long computational time is still unacceptable for the use in the design optimisation process. Consequently, a single-phase hybrid 2D axisymmetric model is proposed to further reduce the computational time while maintaining an acceptable accuracy required by the manufacturing company.

The model enables a magnetic field analysis for multiple cross-sections to simulate the variety of transformer geometries around the winding circumference. The windings are therefore divided into four sections (Figure 6). For the three-limb transformers, the magnetic field of two different sections is analysed (sections a and b in Figure 6). The total eddy current losses are then calculated by considering the section proportion to the circumference of the conductor. Such an approach takes into account the yoke and tank effect on the magnetic field distribution. For a five-limb transformer design, the third cross-section (section c in Figure 6) is analysed to determine the effect of the side limb on the stray magnetic field.

The comparison of the results for the detailed 3D model (Table 2; total losses 35.5 kWh) and the hybrid 2D model (Table 3; total losses 36.7 kWh) shows, that the difference in the calculated total eddy current losses is 3.4%.

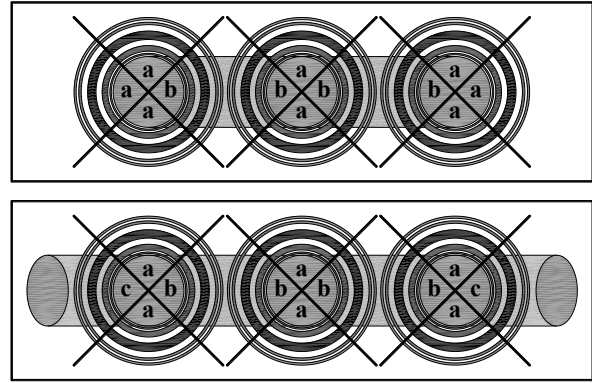


Figure 6. Three-limb (above) and five-limb (below) transformer sections for the 2D eddy current losses calculation – a) tank effect; b) yoke effect; c) side-limb effect.

Table 2: Winding eddy current losses for transformer no. 12
A – Detailed 3D transformer model
B – Simplified 3D transformer model

Winding	Radial eddy current losses [kW]		Axial eddy current losses [kW]		Winding eddy current losses [kW]	
	A	B	A	B	A	B
Tertiary	1.4	1.4	0.1	0.0	1.5	1.4
Low-voltage	2.7	2.7	11.5	12.2	14.2	14.9
High-voltage	1.7	1.5	15.9	15.5	17.6	17.0
Coarse	0.5	0.4	1.5	1.3	2.0	1.7
Fine	0.0	0.0	0.2	0.2	0.2	0.2
Total losses	6.3	6.0	29.2	29.2	35.5	35.2

Table 3: Winding eddy current losses for transformer no. 12
Hybrid 2D transformer model

Winding	Radial eddy current losses [kW]		Axial eddy current losses [kW]		Winding eddy current losses [kW]	
	hybrid	classic	hybrid	classic	hybrid	classic
Tertiary	1.5	1.2	0.0	0.0	1.5	1.2
Low-voltage	2.9	2.3	11.4	11.9	14.3	14.2
High-voltage	1.4	1.4	16.4	17.3	17.8	18.7
Coarse	0.4	0.3	2.5	2.8	2.9	3.1
Fine	0.0	0.0	0.2	0.2	0.2	0.2
Total losses	6.2	5.2	30.5	32.2	36.7	37.4

This is acceptable for a practical estimation of the total transformer losses. The advantage of the described hybrid 2D model is that it provides a valid result with a reduced computational time, depending on the mesh size and its number of the finite elements. While maintaining the adaptive meshing settings, the number of finite elements for the hybrid solution is significantly lower than for the simplified 3D model. By using the 2D model of the transformer no. 12, the solution is analysed with $1.2 \cdot 10^5$ finite elements. Traditionally, only one cross-section of the transformer is analysed. Based on the distribution of the stray magnetic field, the eddy current losses are integrated over the volume of all the windings. The results of this approach are presented

in Table 3 in the columns labelled “classic”. Section b (Figure 6) is used for the analysis. Due to the yoke effect, the axial eddy current losses are predictably higher than those of the hybrid model. Alternatively, the radial eddy current losses are slightly lower due to the predominance of the axial component of the stray magnetic flux path at the winding ends. Overall, for the given transformer geometry (transformer no. 12), the calculated total eddy current losses when analysing only one cross-section (37.4 kWh) are by 5.4% higher than the losses calculated using the detailed 3D model (35.5 kWh).

Table 4 shows the winding eddy current losses for the entire set of 14 transformers. The results of the 2D hybrid model are not significantly different from the results of the 3D model. Therefore, the hybrid 2D model is used to evaluate the increase in the windings eddy current losses when the transformer is exposed to GIC. Table 4 shows the calculated eddy current losses at the occurrence of 33.5 A/phase and 67 A/phase GIC. Under GIC conditions, when the transformer core is completely saturated, the path of the stray flux in the transformer is even more determined by the structural elements. By using the proposed hybrid 2D model, these elements can easily be incorporated with just a slight increase in the mesh size.

3.2 Circulating Current Losses of the Transformer Windings

The circulating current losses in normal and GIC conditions (Table 5) are calculated only for the transformers (Table 1) that carry coils wound with rectangular parallel conductors. The rest of the modelled transformers are wound with the continuously transposed cable, which inherently eliminates the circulating current effect. Due to the requirements of a highly detailed winding model (Figure 4), which consequently leads to a significant increase in the number of the finite elements, the 2D *xy*-plane geometry with a transient solution is used. This geometry is not ideal for studying the winding losses, as it does not represent all of the stray magnetic field conditions around the winding circumference. These results are therefore intended as a guide to predicting short-circuit losses for a particular transformer design.

Figure 7 presents the load current distribution through the parallel conductors of the low-voltage winding of the transformer no. 3 (Table 1), using the transposition scheme from Figure 3. The currents through the parallel conductors are obtained by simulating a short-circuit test. The transformer model is energized at the rated current on the high-voltage side with the rated tap position.

Table 4: Winding eddy current losses increase due to GIC

Tr. no.	Total 3D eddy current losses [kW]	Total 2D eddy current losses [kW]	Total 2D eddy current losses [kW] GIC = 33.5 A	Total 2D eddy current losses [kW] GIC = 67 A
1	2.6	2.7	3.9	6.5
2	3.3	3.4	4.5	6.1
3	3.3	3.3	6.5	11.5
4	4.6	4.5	7.3	12.2
5	8.0	8.1	9.1	12.8
6	6.1	5.9	10.2	15.1
7	9.6	9.8	14.5	21.6
8	11.5	11.2	12.8	16.5
9	16.6	16.2	17.8	20.0
10	20.8	18.9	20.9	22.9
11	16.5	16.3	19.7	25.4
12	35.5	36.7	39.7	44.8
13	35.7	33.5	39.7	45.0
14	47.1	47.3	48.3	51.8

Table 5: Winding circulating current losses XY-plane 2D transformer model

Tr. no.	Circulating current losses [kW]	Circulating current losses [kW] GIC = 33.5 A	Circulating current losses [kW] GIC = 67 A
3	1.0	1.5	2.0
4	0.8	1.0	1.2
5	1.0	1.1	1.2
6	1.0	1.2	1.5
7	1.0	1.2	1.4

The used transposition scheme is valid for symmetrical magnetic field conditions with regard to the centre of the winding. If there is a large difference between the distances of the winding to the top and to the bottom yoke, the stray flux paths at the ends of the winding will be different and the evenly spaced transposition of the parallel conductors will need to be revised. This difference is unavoidable due to the transformer manufacturing processes and is between 10% and 20% for the low power range transformers with rectangular conductors. In order to evaluate the transposition scheme under these conditions, the winding positions of the transformer no. 3 are modified to take into account the 20% difference between the upper and lower winding distances from the yoke. The results of the circulating current losses for this modification are shown in Table 6. Comparison of the simulation results with those for the centrally positioned windings (Table 5) shows that the differences are negligible and the chosen transposition scheme is appropriate.

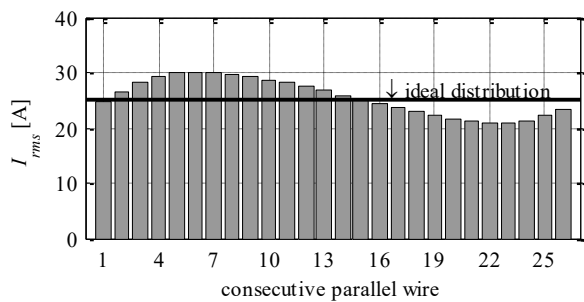


Figure 7. Distribution of the load current through the low-voltage winding parallel conductors (transformer no. 3).

Table 6: Winding circulating current losses
The XY-plane 2D transformer model with the windings offset from the centre

Tr. no.	Circulating current losses [kW]	Circulating current losses [kW] GIC = 33.5 A	Circulating current losses [kW] GIC = 67 A
3	1.0	1.5	2.1

4 CONCLUSION

A hybrid 2D transformer model is presented to evaluate the winding eddy current losses. Compared to a detailed 3D model used as a reference, the proposed modelling solution significantly reduces the mesh size (by a factor of 10) with an acceptable decrease in the accuracy of the calculated magnetic field distribution in the power transformer. A transformer designer can therefore use the proposed calculation procedure on a regular basis.

A hybrid 2D model is also used to evaluate the winding losses in the presence of GIC. It is shown that GIC contribute to a substantial increase in the winding losses. Consequently, transformer designers should adjust the transformer geometry and eventually use some additional construction elements to make the transformer more robust to the GIC phenomenon. As to the circulating current losses, there is a further increase in the additional winding losses for the transformers wound with parallel rectangular conductors, especially when subjected to GIC.

In the future, additional laboratory measurements beyond standard tests will be conducted to verify the simulation results. The proposed eddy current loss calculation procedure will thus be fully implemented, providing an efficient tool in the design of power transformers.

ACKNOWLEDGMENTS

The research was supported by the Slovenian Research and Innovation Agency through the research programme “Electric Power Converters and Controlled Drives” (grant no. P2-0258).

REFERENCES

- [1] C. A. Charalambous, A. Milidonis, A. Lazari, and A. I. Nikolaidis, “Loss Evaluation and Total Ownership Cost of Power Transformers-Part I: A Comprehensive Method,” *IEEE Trans. Power Deliv.*, vol. 28, no. 3, pp. 1872–1880, Jul. 2013.
- [2] P. S. Georgilakis, “Recursive Genetic Algorithm-finite Element Method Technique for the Solution of Transformer Manufacturing Cost Minimisation Problem,” *IET Electr. Power Appl.*, vol. 3, no. 6, pp. 514–519, Nov. 2009.
- [3] E. I. Amoiralis, M. A. Tsili, D. G. Paparigas, and A. G. Kladas, “Global Transformer Design Optimization Using Deterministic and Nondeterministic Algorithms,” *IEEE Trans. Ind. Appl.*, vol. 50, no. 1, pp. 383–394, Jan. 2014.
- [4] M. A. Arjona, C. Hernandez, and M. Cisneros-Gonzalez, “Hybrid Optimum Design of a Distribution Transformer Based on 2-D FE and a Manufacturer Design Methodology,” *IEEE Trans. Magn.*, vol. 46, no. 8, pp. 2864–2867, Aug. 2010.
- [5] L. D. S. Coelho, V. C. Mariani, F. A. Guerra, M. V. F. da Luz, and J. V. Leite, “Multiobjective Optimization of Transformer Design Using a Chaotic Evolutionary Approach,” *IEEE Trans. Magn.*, vol. 50, no. 2, pp. 669–672, Feb. 2014.
- [6] M. A. Tsili, E. I. Amoiralis, A. G. Kladas, and A. T. Souflaris, “Optimal Design of Multi-winding Transformer Using Combined FEM, Taguchi and Stochastic-deterministic Approach,” *IET Electr. Power Appl.*, vol. 6, no. 7, pp. 437–454, Aug. 2012.
- [7] E. I. Amoiralis, M. A. Tsili, and A. G. Kladas, “Transformer Design and Optimization: A Literature Survey,” *IEEE Trans. Power Deliv.*, vol. 24, no. 4, pp. 1999–2024, Oct. 2009.
- [8] M. Vitelli, “Numerical Evaluation of 2-D Proximity Effect Conductor Losses,” *IEEE Trans. Power Deliv.*, vol. 19, no. 3, pp. 1291–1298, Jul. 2004.
- [9] S. V. Kulkarni, *Transformer engineering: design, technology, and diagnostics*, 2nd ed. Boca Raton: CRC Press, 2013.
- [10] R. M. Del Vecchio, Ed., *Transformer design principles: with applications to core-form power transformers*, 2nd ed. Boca Raton, FL: CRC Press, 2010.
- [11] L. Kralj and D. Miljavec, “Stray Losses in Power Transformer Tank Walls and Construction Parts,” in *2010 XIX International Conference on Electrical Machines (ICEM)*, 2010, pp. 1–4.
- [12] S. V. Kulkarni, J. C. Olivares, R. Escarela-Perez, V. K. Lakhiani, and J. Turowski, “Evaluation of Eddy Current Losses in the Cover Plates of Distribution Transformers,” *Sci. Meas. Technol. IEE Proc.*, vol. 151, no. 5, pp. 313–318, Sep. 2004.
- [13] G. B. Kumbhar, S. M. Mahajan, and W. L. Collett, “Reduction of Loss and Local Overheating in the Tank of a Current Transformer,” *IEEE Trans. Power Deliv.*, vol. 25, no. 4, pp. 2519–2525, Oct. 2010.
- [14] R. Escarela-Perez, S. V. Kulkarni, J. Alvarez-Ramirez, and K. Kaushik, “Analytical Description of the Load-Loss Asymmetry Phenomenon in Three-Phase Three-Limb Transformers,” *IEEE Trans. Power Deliv.*, vol. 24, no. 2, pp. 695–702, Apr. 2009.
- [15] ANSYS Maxwell. ANSYS, Inc.
- [16] D. Meeker, *FEMM: Finite Element Method Magnetics*.
- [17] K. Zheng, D. Boteler, R. J. Pirjola, L. Liu, R. Becker, L. Marti, S. Boutilier, and S. Guillon, “Effects of System Characteristics on Geomagnetically Induced Currents,” *IEEE Trans. Power Deliv.*, vol. 29, no. 2, pp. 890–898, Apr. 2014.
- [18] R. Horton, D. H. Boteler, T. J. Overbye, R. Pirjola, and R. C. Dugan, “A Test Case for the Calculation of Geomagnetically Induced Currents,” *IEEE Trans. Power Deliv.*, vol. 27, no. 4, pp. 2368–2373, Oct. 2012.
- [19] E. Bernabeu, “Modeling Geomagnetically Induced Currents in Dominion Virginia Power Using Extreme 100-Year Geoelectric Field Scenarios-Part 1,” *IEEE Trans. Power Deliv.*, vol. 28, no. 1, pp. 516–523, Jan. 2013.

- [20] L. Marti, A. Rezaei-Zare, and A. Narang, "Simulation of Transformer Hotspot Heating due to Geomagnetically Induced Currents," *IEEE Trans. Power Deliv.*, vol. 28, no. 1, pp. 320–327, Jan. 2013.
- [21] L. Marti, J. Berge, and R. K. Varma, "Determination of Geomagnetically Induced Current Flow in a Transformer From Reactive Power Absorption," *IEEE Trans. Power Deliv.*, vol. 28, no. 3, pp. 1280–1288, Jul. 2013.
- [22] P. R. Price, "Geomagnetically Induced Current Effects on Transformers," *IEEE Trans. Power Deliv.*, vol. 17, no. 4, pp. 1002–1008, Oct. 2002.
- [23] A. Rezaei-Zare, "Behavior of Single-Phase Transformers Under Geomagnetically Induced Current Conditions," *IEEE Trans. Power Deliv.*, vol. 29, no. 2, pp. 916–925, Apr. 2014.
- [24] R. Girgis and K. Vedante, "Methodology for Evaluating the Impact of GIC and GIC Capability of Power Transformer Designs," in *2013 IEEE Power and Energy Society General Meeting (PES)*, 2013, pp. 1–5.
- [25] R. J. Pirjola, A. T. Viljanen, and A. A. Pulkkinen, "Research of Geomagnetically Induced Currents (GIC) in Finland," in *2007 7th International Symposium on Electromagnetic Compatibility and Electromagnetic Ecology*, 2007, pp. 269–272.
- [26] R. S. Girgis, D. J. Scott, D. A. Yannucci, and J. B. Templeton, "Calculation of Winding Losses in Shell-Form Transformers for Improved Accuracy and Reliability Part-1: Calculation Procedure and Program Description," *IEEE Trans. Power Deliv.*, vol. 2, no. 2, pp. 398–403, Apr. 1987.
- [27] Ž. Janic, Z. Valkovic, and Ž. Štih, "Helical Winding's Magnetic Field in Power Transformers," *Electr. Eng.*, vol. 91, no. 3, pp. 161–166, Nov. 2009.
- [28] B. Stojčić and D. Miljavec, "Current Distribution in the Low-voltage Winding of the Furnace Transformer," *Int. J. Electr. Power Energy Syst.*, vol. 43, no. 1, pp. 1251–1258, Dec. 2012.
- [29] H. J. Kaul, "Stray-Current Losses in Stranded Windings of Transformers," *Power Appar. Syst. Part III Trans. Am. Inst. Electr. Eng.*, vol. 76, no. 3, pp. 137–146, Apr. 1957.
- [30] S. Isaka, T. Tokuinasu, and K. Kondo, "Finite Element Analysis of Eddy Currents in Transformer Parallel Conductors," *IEEE Trans. Power Appar. Syst.*, vol. PAS-104, no. 10, pp. 2730–2737, Oct. 1985.

Peter Kosmatin received his B.Sc. and Ph.D. degrees from the University of Ljubljana, Faculty of Electrical Engineering, Slovenia, in 2006 and 2012, respectively. He is currently employed at Kolektor Etra, a power transformer manufacturer located in Ljubljana, Slovenia, where he works as a power transformer designer.

David Nedeljković received his B.Sc., M.Sc., and Ph.D. degrees from the University of Ljubljana, Faculty of Electrical Engineering, Slovenia, in 1991, 1996, and 1998, respectively. In 1993, he joined the same faculty where he is currently employed as an Associate Professor and Vice Dean for Quality and Sustainable Development. His research interests include active power filters, power converters, electric vehicles, and control of electrical drives.